SUPPLEMENTAL INFORMATION INVENTORY

I. Supplementary Figures

Supplementary Figure 1. Tetraploid cells activate p53 via mechanisms that are independent of DNA damage. Related to Figure 1.

Supplementary Figure 2. Hyperactivation of growth factor signaling bypasses general low-level p53 activation. Related to Figure 2.

Supplementary Figure 3. Tetraploid cells activate the Hippo pathway. Related to Figure 3.

Supplementary Figure 4. Loss of p53 or constitutive activation of YAP both overcome tetraploid-induced cell cycle arrest. Related to Figure 4.

Supplementary Figure 5. Tetraploid proliferation can be rescued by either activating RhoA or inhibiting Rac. Related to Figure 5.

Supplementary Figure 6. Tetraploid hepatocytes activate the HIPPO pathway. Related to Figure 6.

Supplementary Figure 7. High-ploidy tumors show frequent *YAP* amplification or *LATS1/2* deletion. Related to Figure 7.

II. Supplementary Movies

Supplementary Movie 1. Related to Figure 1. Live-cell imaging of FACS-sorted G_1 diploid RPE-1 FUCCI cells following 16 h of exposure to DCB. Upon attachment, cells were transfected with scrambled siRNA and imaged for ~48 hr.

Supplementary Movie 2. Related to Figure 1. Live-cell imaging of FACS-sorted G_1 binucleated tetraploid RPE-1 FUCCI cells following 16 h of exposure to DCB. Upon attachment, cells were transfected with scrambled siRNA and imaged for ~48 hr.

Supplementary Movie 3. Related to Figure 1. Live-cell imaging of FACS-sorted G_1 binucleated tetraploid RPE-1 FUCCI following 16 h of exposure to DCB. Upon attachment, cells were transfected with p53 siRNA and imaged for ~48 hr. Related to Figure 1.

III. Supplementary Tables

Supplementary Table 1. Related to Figure 1. Gene hits from the secondary, deconvolved tetraploid RNAi screen. The number of individual siRNAs (out of 4) that significantly induced tetraploid cell proliferation per gene are shown. Related to Figure 1.

Supplementary Table 2. Related to Figure 1. Gene hits identified from the primary DNA damage RNAi screen. Related to Figure 1.

IV. Extended Experimental Procedures

V. Supplementary References

SUPPLEMENTAL FIGURE LEGENDS

Supplementary Figure 1. Tetraploid cells activate p53 via mechanisms that are independent of DNA damage. Related to Figure 1. (A) Diploid (arrowheads) and binucleated tetraploid (arrows) cells expressing Cdt1-mCherry and GFP-Azami Green, stained for p53 (yellow) and DNA (blue). Quantitative immunofluorescence was used to determine the mean fluorescence intensity of p53 in individual nuclei. **(B)** The average intensity of p53 fluorescence in tetraploid cells relative to diploid cells over time. Data from two independent experiments are shown. **(C)** Right: The fraction of binucleated tetraploid cells (4N) generated by DCB treatment that exhibit β-galactosidase activity after the indicated times in culture, relative to baseline levels in diploid cells (2N). Left: A representative DIC image of a binucleated tetraploid cell, which exhibits β-galactosidase activity (white arrow). **(D)** The percentage of S/G_2 diploid (2N) and tetraploid (4N) RPE-FUCCI cells upon treatment with the indicated concentrations of N-acetyl cysteine (NAC) for 48 h. **(E)** Still images from a live-cell imaging experiment of tetraploid RPE-FUCCI cells generated by Ect2 siRNA or 100 μM Hesperadin, and diploid controls (2N). Time, h:minutes. Scale bar, 100 μm. Right: Quantitation of the total number of cells that enter S-phase after 24 h. **(F)** Freshly sorted diploid (2N) and tetraploid (4N) RPE-FUCCI cells in G_1-phase (as judged by Cdt1-mCherry fluorescence) stained for γ-H2AX (yellow). Cells treated with 40 ng/ml doxorubicin (+Dox) are positive controls. Cells exhibiting one or more γ-H2AX foci were considered γ-H2AX positive. Right: Quantitation of the fraction of γ-H2AX positive diploid (2N) and tetraploid (4N) cells at various time points following their geration (n=3). Scale bar, 25 μm.

Supplementary Figure 2. Hyperactivation of growth factor signaling bypasses general low-level p53 activation. Related to Figure 2. (A) Protocol for genome-wide RNAi screen to identify genes necessary to activate or maintain G_1 cell cycle arrest in cells with low level DNA damage. **(B)** A

representative western blot of phosphorylated ERK1/2, and total ERK1/2 at time points (in min) following addition of serum to starved cells that are transfected with the indicated siRNAs. Right: quantitation of phosphorylated ERK1/2 relative to total ERK1/2.

Supplementary Figure 3. Tetraploid cells activate the Hippo pathway. Related to Figure 3. (A) The percentage of S/G_2 tetraploid RPE-1 FUCCI cells following transfection with the indicated siRNAs after 72 h (n=2). Below: Analysis of knockdown efficiency for each siRNA. Because the LATS2 antibody used in this experiment (Bethyl) also detects LATS1, we co-depleted LATS1 to better visualize remaining levels of LATS2. Note that the ability to bypass cell cycle arrest is well correlated with LATS2 knockdown. **(B)** Knockdown efficiency for individual siRNAs against the LATS2 3'UTR also correlates with release from tetraploid arrest. **(C)** The percentage of S/G_2 tetraploid RPE-FUCCI cells following transfection with the indicated pooled siRNAs after 72 h (n=4; *$p < 0.03$, one sample t-test). **(D)** The percentage of S/G_2 tetraploids cells (generated by ECT2 or PRC1 siRNA) after co-transfection with negative control siRNA (siControl) or LATS2 siRNA. Error bars represent the mean ± SEM from at least 3 independent experiments; *$p < 0.02$, unpaired t-test. **(E)** Western analysis (top) and quantitation (bottom) of the amount of phosphorylated-YAP to total YAP in subconfluent diploid (2N) and tetraploid (4N) cells relative to diploid cells grown to confluence (dense). Error bars represent the mean ± SEM from 4 independent experiments; *$p < 0.05$, paired t-test. **(F)** Diploid (2N) and binucleated tetraploid (4N) RPE-1 cells generated by ECT2 depletion were stained for YAP. Quantitation of YAP distribution from two independent experiments distribution is shown: N > C: YAP enriched in the nucleus; N = C: YAP evenly distributed; N < C: YAP enriched in the cytoplasm (n=2). **(G)** The effect of tetraploidy on YAP phosphorylation is not explained by cell cycle position effects. Freshly isolated diploid (2N) and tetraploid (4N) RPE-1 FUCCI cells were serum-starved for 18 h to synchronize cells in G_0, and then released into G_1 by addition of serum for 6 h before analyzing YAP distribution. Quantitation of two independent experiments is shown. **(H)**

Freshly isolated diploid (2N) and tetraploid (4N) RPE-1 FUCCI cells were serum-starved for 18 h to synchronize cells in G_0, and then released into G_1 by addition of serum for 6 h before analyzing YAP phosphorylation. Quantitation from two independent experiments is shown. Error bars represent the mean ± SEM. **(I)** Western blot analysis of Hippo pathway activity in diploid (2N) and tetraploid (4N) cells following transfection with the indicated siRNAs for 48 h.

Supplementary Figure 4. Loss of p53 or constitutive activation of YAP both overcome tetraploid-induced cell cycle arrest. Related to Figure 4. (A) RPE-1 cells transfected with the indicated siRNAs and analyzed by immunofluorescence for YAP localization (green). Scale bar, 50 μm. **(B)** Western blot analysis of RPE-1 FUCCI cells stably expressing the indicated versions of YAP. **(C)** The percentage of S/G_2 tetraploids (generated by ECT2 or PRC1 siRNA) in RPE-1 cells expressing YAP-S5A or empty-vector (Control). Error bars represent the mean ± SEM from 4 independent experiments; *$p < 0.001$, unpaired t-test. **(D)** Western blot of p53 levels in RPE-1 FUCCI cells stably expressing the indicated versions of YAP following treatment with or without 40 ng/ml doxycycline. **(E)** Western blot analysis and corresponding quantitation of p53 levels in diploid (2N) and tetraploid (4N) RPE-1 FUCCI cells 72 h after transfection with the indicated siRNAs (n=3; *$p < 0.004$, unpaired t-test). Error bars represent the mean ± SEM. **(F)** The percentage of S/G_2 tetraploid RPE-1 FUCCI cells 72 h after transfection with the indicated siRNAs. Error bars represent the mean ± SEM from 2 independent experiments. Below: Confirmation of MST1 and MST2 knockdown following transfection with the indicated siRNAs. **(G)** Diploid (2N) and binucleated tetraploid (4N) RPE-1 cells stained for actin (red), microtubules (green), and DNA (blue). Scale bar, 50 μm. (**H**) Western blot analysis of phosphorylated myosin light chain (P-MLC) and total myosin light chain (MLC) in diploid (2N) and tetraploid (4N) cells. Quantitation of P-MLC relative to total MLC is shown in the panel below. Error bars represent the mean ± SEM from 6 independent experiments; *$p < 0.0005$, one-sample t-test).

Supplementary Figure 5. Tetraploid proliferation can be rescued by either activating RhoA or inhibiting Rac. Related to Figure 5. (A) Total cell area (left) and total mechanical energy (right) displayed as scatter-plots for individual diploid (2N), freshly generated tetraploid (4N), and evolved tetraploid (4N Evolved) cells. The total mechanical energy each cell transmitted onto the underlying substrate was calculated by summing the local traction forces. Despite their larger size, freshly generated tetraploids do not display a significant increase in mechanical energy relative to diploids. By contrast, evolved tetraploid cells, which have adapted to overcome Hippo pathway activation and have a normal number of centrosomes, display significant increases in both cell size and mechanical energy. 2N and 4N data points are from 4 independent experiments; 4N Evolved data points are from 2 independent experiments; *$p < 0.0001$, unpaired t-test. **(C)** The percentage of S/G_2 tetraploid RPE-FUCCI cells following 48 h of treatment with 1 μM LPA or S1P. Error bars represent the mean ± SEM from 5 independent experiments; *$p < 0.0001$, unpaired t-test. **(D)** The percentage of S/G_2 RPE-1 FUCCI cells grown in the continuous presence of 40 ng/ml doxorubicin after 48 h treatment with 1 μM LPA, S1P, or 10 μM ATM inhibitor. Error bars represent the mean ± SEM from 2 independent experiments. **(E)** The percentage of S/G_2 tetraploid RPE-FUCCI cells generated by ECT2 siRNA following treatment with ± 1 μM S1P, or 5 μM of the Rac inhibitors NSC2376 and EHT1864. Error bars represent the mean ± SEM from 4 independent experiment; *$p < 0.05$, unpaired t-test. **(F)** The percentage of S/G_2 RPE-1 FUCCI grown in the continuous presence of 40 ng/ml doxorubicin after 48 h treatment with 5 μM of the Rac inhibitors NSC2376 and EHT1864, or 1 nM Taxol. Error bars represent the mean ± SEM from 4 independent experiments.

Supplementary Figure 6. Tetraploid hepatocytes activate the HIPPO pathway. Related to Figure 6. (A) Overview of the gene sets used for GSEA analysis of diploid and tetraploid hepatocytes. These

gene sets represent a "Hippo-Off/Yap-On" gene signature. The Hippo Liver signature was constructed as described in the Extended Experimental Procedures. **(B)** Graphical representation of GSEA results comparing the gene expression profiles of diploid and tetraploid hepatocytes to the two "Hippo-Off/Yap-On" gene sets. Each vertical black line represents a unique gene from the "Hippo-Off/Yap-On" gene set and its relative expression in diploid (red-shifted) or tetraploid (blue shifted) hepatocytes. **(C)** qPCR analysis of hYAP and mCTGF expression levels in YFP^{+} murine hepatocytes treated ± doxycycline to induce hYAP expression (n=3; *p < 0.0001, unpaired t-test). All error bars represent mean ± SEM.

Supplementary Figure 7. High-ploidy tumors show frequent *YAP* amplification or *LATS1/2* deletion. Related to Figure 7. (A) Diploid (2N), freshly generated tetraploid (4N), and evolved tetraploid (evolved) cells were stained for YAP and its distribution was quantified (N > C: YAP enriched in the nucleus; N = C: YAP evenly distributed; N < C: YAP enriched in the cytoplasm). **(B)** Western blot of phosphorylated p53 (p-S15) in diploid (2N) and evolved tetraploid (Evolved 4N) RPE-1 cells, before and after treatment with 100 ng/ml doxorubicin. **(C)** Western blot of endogenous YAP from control $p53^{-/-}$ mouse mammary epithelial cells and tetraploid-derived tumors from 5 mice. **(D-F)** A pool of 475 cell lines from the Cancer Cell Line Encyclopedia (CCLE), for which ploidy-status was available (Carter et al., 2012), were initially categorized according to the genomic status of *YAP*, *LATS1* and *LATS2*. Genes were considered to have no amplification/deletion if the DNA copy number was (log2 ratio) = -0.5 – 0.3; to be amplified if the DNA copy number was > 0.3; to be deleted if the DNA copy number < -0.5). Resulting samples were then classified based on their respective ploidy. **(D)** Analysis for *YAP* (n=292; *p < 0.0001, Mann-Whitney Test; **p < 0.002, 2-way ANOVA); **(E)** *LATS2* (n=184; *p < 0.015, Mann-Whitney Test; **p < 0.03, 2-way ANOVA); and **(F)** *LATS1* (n=183; *p < 0.001, Mann-Whitney Test; **p < 0.002, 2-way ANOVA).

Supplementary Movie 1. Related to Figure 1. Live-cell imaging of FACS-sorted G_1 diploid RPE-1 FUCCI cells following 16 h of exposure to DCB. Upon attachment, cells were transfected with scrambled siRNA and imaged for ~48 hr.

Supplementary Movie 2. Related to Figure 1. Live-cell imaging of FACS-sorted G_1 binucleated tetraploid RPE-1 FUCCI cells following 16 h of exposure to DCB. Upon attachment, cells were transfected with scrambled siRNA and imaged for ~48 hr.

Supplementary Movie 3. Related to Figure 1. Live-cell imaging of FACS-sorted G_1 binucleated tetraploid RPE-1 FUCCI following 16 h of exposure to DCB. Upon attachment, cells were transfected with p53 siRNA and imaged for ~48 hr.

Supplementary Table 1. Related to Figure 1. Gene hits from the secondary, deconvolved tetraploid RNAi screen. The number of individual siRNAs (out of 4) that significantly induced tetraploid cell proliferation per gene are shown.

Supplementary Table 2. Related to Figure 1. Gene hits identified from the primary DNA damage RNAi screen.

EXTENDED EXPERIMENTAL PROCEDURES

Cell Culture

Telomerase-immortalized RPE-1 cells (ATCC), and all derivative cell lines generated in this study, were grown in phenol red-free DMEM:F12 media containing 10% FBS, 100 IU/ml penicillin, and 100 μg/ml streptomycin. All cells were maintained at 37°C with 5% CO_2 atmosphere.

Viral Infections and siRNA Transfections

RPE-1 cells were infected for 12-16 h with virus carrying genes of interest (generated as described in Extended Experimental Procedures) in the presence of 10 μg/ml polybrene, washed, and allowed to recover for 24 h before selection. All siRNA transfections were performed using 50 nM siRNA with Lipofectamine RNAi MAX according the manufacturer's instructions.

Tetraploid RNAi Screen

Day 1: Fifteen cm dishes were seeded with 6 million exponentially growing RPE-FUCCI cells, such that they were ~65% confluent the following day. **Day 2**: 4 μM DCB was added to each 15 cm dish for 16 h. **Day 3**: DCB-treated cells were washed 5 X 5 min, incubated in medium containing 2.5 μg/ml Hoechst dye for 1 h, then trypsinized in 0.05% trypsin and G_1 diploids (2C DNA content; $mCherry^+$, GFP^-) and G_1 tetraploids (4C DNA content; $mCherry^+$, GFP^-) and isolated by FACS sorting. Sorted cells were pelleted, re-suspended in fresh medium without antibiotics, and re-plated at a density of 5000 cells per well of a 384-well plate; they were then reverse-transfected using Lipofectamine RNAi Max (according to the manufacturer's specifications). The final concentration of siRNAs per well was 50 nM. Each plate was screened in triplicate, and was internally controlled with multiple p53 siRNA-

positive controls and scrambled siRNA negative controls. **Day 4**: All transfected wells were fed with fresh medium containing penicillin/streptomycin. **Day 6**: 100 μM monastrol was added to each well for 12 h, to arrest proliferating GFP^+ cells in mitosis. **Day 7**: 96 h following transfection, cells were fixed with 4% paraformaldehyde. Automated fluorescence microscopy using a Nikon TE2000-E2 inverted microscope equipped with a cooled CCD camera (Orca ER, Hamamatsu) and Nikon Perfect Focus, and a precision stage was used to capture 9 fields of view from each well of the 384-well dish. Subsequently, the total number of proliferating $S/G_2/M$ cells (based on GFP positivity of the FUCCI system) was calculated as a fraction of the total number of cells (based on nuclear counts using Hoechst) for each well. All pooled siRNAs that had a median Z-score of 2.0 were deconvolved and individual siRNAs were tested in a secondary screen, following the same protocol as for the primary screen.

DNA Damage RNAi Screen. This screen was similar to the tetraploid screen, but with four notable differences: i) instead of DCB, cells were treated with 40 ng/ml doxorubicin for the duration of the experiment; ii) G_1 cells (RFP^+, GFP^-) were FACS-purified without Hoechst treatment; iii) no monastrol was added during the final 12 h of the experiment; and iv) image analysis was performed with a laser scanning cytometer (ImageXpress Velos), rather than a microscope, at 24, 48, 72 and 96 h post-transfection. The selection of hits from the DNA damage screen was done by using robust z-score (z=(sample value-sample median)/(sample median absolute deviation)) for normalization. A gene was considered a hit if it was > 5*MAD (median absolute deviation).

Microarray Analysis and GSEA

Total RNA was extracted from exponentially growing diploid and evolved tetraploid RPE-1 cells, or from FACS-sorted diploid and tetraploid primary murine hepatocytes (see below for details), with the

RNeasy kit (Qiagen) and was hybridized onto the Affymetrix HG-U133_Plus_2 arrays as per the manufacturer's instruction. Gene set enrichment analysis (GSEA) was performed using gene sets as permutation type, 1,000 permutations and $\log_2$ ratio of classes as metric for ranking genes. Published Gene sets used are shown in Figure S6. For the analysis of murine hepatocytes, all probe IDs were converted to the corresponding MOE430A 2.0 probe sets, making use of the NetAffx orthologue annotation file derived from the NCBI HomologoGene database (MOE430A Orthologues/Homologues Release 30, http://www.affymetrix.com/). To construct the HIPPO Liver gene-set, we used genes that were commonly upregulated in murine liver that overexpressed YAP (Dong, Cell, 2007) or was deficient for MST1/2 and SAV1 (Lu, PNAS, 2010).

Immunofluorescence Microscopy

All cells were washed in PBS and fixed in 4% paraformaldehyde for 10 min. Cells were extracted in PBS-0.5% Triton X-100 for 5 min., blocked for 30 min in TBS-BSA (10 mM Tris, pH 7.5, 150 mM NaCl, 5% BSA, 0.2% sodium azide), and incubated with primary antibodies diluted in TBS-BSA for 30-60 min in a humidified chamber. Primary antibodies were visualized using species-specific fluorescent secondary antibodies (Molecular Probes) and DNA was detected with 2.5 µg/ml Hoechst. Immunofluorescence images were collected with a Yokogawa CSU-X1 spinning disk confocal (Andor Technology) mounted on a Nikon Ti-E inverted microscope (Nikon Instruments). Immunofluorescence images of RPE-FUCCI cells, including all data collected from the RNAi screen, were captured on a Nikon TE2000-E2 inverted microscope. Images were analyzed using NIS-Elements software.

Live-cell Imaging

RPE-FUCCI cells were grown on glass-bottom 12-well tissue culture dishes (Mattek) and imaged on a Nikon TE2000-E2 inverted microscope equipped with the Nikon Perfect Focus system. The microscope was enclosed within a temperature- and CO_2-controlled environment that maintained an

atmosphere of 37°C and 3-5% humidified CO_2. Fluorescence and phase contrast images were captured every 10-20 minutes with a 10X 0.5 NA Plan Fluor objective, at multiple points for 2-4 days. All captured images were analyzed using NIS-Elements software.

Protein Extraction, Immunoprecipitation and Immunoblotting

Cells were washed twice in ice-cold PBS and lysed using ice-cold RIPA buffer containing protease (Roche) and phosphatase (Pierce) inhibitors. Lysates were incubated for 20 min on ice, centrifuged at 14,000 x g at 4 °C for 15 min, and resolved using SDS gel electrophoresis. Proteins were then transferred onto PVDF membranes, blocked for 1 h with TBS-0.5% Tween containing 5% skim milk powder, and then probed overnight at 4° C with primary antibodies. Bound antibodies were detected by horseradish peroxidase-linked secondary antibodies and processed with ECL or ECL Prime (Amersham). Quantification of chemiluminescence was carried out using the Image Quant LAS 4000 system (GE Healthcare). For immunoprecipitations, cells were lysed in NP-40 lysis buffer (50 mM Tris-HCl at pH 8.0, 150 mM NaCl, 1.0% NP-40, containing protease and phosphatase inhibitors) and centrifuged as above. Samples were pre-cleared with Protein A-sepharose and rabbit control antibody for 1h at 4° C before immunoprecipitation of HA-tagged proteins with anti-HA sepharose (Cell Signaling Technology, #3956) for 4h at 4° C. Beads were then washed 3 times with lysis buffer before SDS-PAGE. SDS-gels containing Phos-Tag were prepared and run according to the manufacturer's instructions (NARD).

hMSC Differentiation Assay

Primary human mesenchymal stem cells (hMSCs, Lonza) maintained in hMSC medium (Lonza) were grown to ~65% confluence and then treated with 4 μM DCB for 16 h; cells were washed for 5 X 5 min and incubated in medium containing 2.5 μg/ml Hoechst dye for 1 h, treated with 0.05% trypsin, and

sorted into two populations based on DNA content (2C and 4C). Both populations of cells were plated at very low densities (~15% confluency) into separate dishes containing a 50:50 mix of both adipocyte and osteogenic differentiation medium (Lonza). After 9-14 days, cells were fixed with paraformaldehyde and stained for adipocytes (Oil Red) and DNA (Hoechst). The total fraction of adipocytes was scored in both the 2C and 4C cell populations. Cells were considered to be diploid if they were mononucleated and in the 2C population, and to be tetraploid if they were binucleated and in the 4C population.

Traction Force Microscopy

Fibronectin coating onto PAA gel was performed by a transfer method adapted from Vignaud et al. (Vignaud et al. Methods in Cell Biology, 2014). Square glass coverslips (20x20mm) were oxidized by exposure to 30 watts oxygen plasma (FEMTO, Diener electronics) for 30 seconds and then incubated in a 40 µg/mL fibronectin solution for 30 min. An acrylamide solution containing acrylamide and bis-acrylamide (8%/0.264%) (Sigma) was degassed for 20 min under vacuum and mixed with PEG-coated red fluorescent beads (Tseng et al., Lab On a Chip, 2011) by sonication. PAA polymerization was triggered by the addition of 1 µL APS (from a 10% w/w stock, Sigma) and 1µL of TEMED (Sigma) in 165µL of acrylamide solution. A 25µL drop of this solution was rapidly put on the fibronectin-coated coverslip and covered with a silanized glass coverslip baring metacrylate moieties (Tseng et al., Lab On a Chip, 2011). After 30 minutes of polymerization, the sandwich was immersed in 100 mM sodium bicarbonate solution in order to help the detachment of the fibronectin-coat with a scalpel. Fibronectin was transfered onto the PAA gel, which remained attached to the silanized glass due to covalent bonds formed with the acrylate groups. PAA coated coverslips were rinsed 3 times with PBS, and incubated for 1h in cell culture medium at 37°C. After trypsinization, 2 X 10^^{4} cells were resuspended in 2 mL of culture medium containing Hoescht at 0.5 µg/mL and plated on the fibronectin-coated PAA gels. Three h after cell plating, the PAA-coated coverslip was mounted in a magnetic observation chamber

(CYTOO) with 1 mL of culture medium (containing Hoechst) and placed on a confocal spinning disk microscope (Nikon) with CO2, humidity and temperature control (Live Cell Instrument). Cell shape was visualized via LifeAct-GFP exposure, nuclear size and number were evaluated using Hoechst, and fluorescent beads positions were recorded by exposure to 561 nm light. Cells were then trypsinized and beads positions were recorded again in order to measure gel relaxation due to the release of traction forces. Force measurement was then performed as described in Tseng et al. (Tseng et al., PNAS, 2012). The deformation field was measured by a custom-written particle image velocimetry. The traction force field was reconstructed by the Fourier transform traction cytometry method with regularized scheme (Sabass et al., Biophys J, 2008) using a PAA gel young modulus estimation of 35 kPa.

Generation of Cell Lines

Lentivirus or retrovirus carrying genes of interest were generated by transfection of 293FT cells, with the appropriate packaging plasmids (Lentivirus: pMD2.G and psPAX2; Retrovirus: pUMVC and pVSV-G) using Lipofectamine 2000, according to the manufacturer's instructions. RPE-1 cells were infected for 12-16 h with virus in the presence of 10 μg/ml polybrene, washed, and allowed to recover for 24 h before selection. To generate the FUCCI cell lines, RPE-1 cells were infected with hCdt1-mCherry and hGem-Azami green, and then FACS-sorted (three times) to purify cells that expressed each fluorophore at the appropriate cell cycle stage, with optimum brightness. To generate RPE-FUCCI cells expressing inducible RhoA-WT and RhoA-Q61L, RPE-1 cells stably expressing the rtTA transactivator (Clontech; pLVX-Tet3G) were generated, and were infected with the doxycycline-inducible constructs. RPE-1 cells expressing doxycycline-inducible PLK4 were kindly provided by Susana Godinho.

Doxycycline-Induced Gene Expression

RPE-1 cells carrying doxycycline-inducible RhoA-WT, RhoA-Q61L, or PLK4, were maintained in medium supplemented with 10% serum that was certified to be tetracycline-free. To induce gene expression, 1 μg/ml doxycycline was added for 20h (RhoA) or 24 h (PLK4).

***In vitro* evolution of tetraploid cells**

Evolved tetraploid RPE-1 cells were derived as described (Ganem et al., 2009). Briefly, tetraploid RPE-1 cells were treated for 16 h with 0.2 μm cytochalasin D, and FACS-sorted by DNA content using Hoechst staining (Molecular Probes). Rare cells with a DNA content of 8C were isolated and cultured for ~1 week before a second FACS sorting was used to re-isolate 8C cells. A total of 5 purifying sorts over the course of ~6 weeks was needed to generate a pure population of proliferating tetraploid cells. Total RNA was extracted from exponentially growing diploid and evolved tetraploid RPE-1 and hybridized onto the Affymetrix HG-U133_Plus_2 arrays as described by the manufacturer.

Growth Factor Re-stimulation

Control RPE-1 cells, or RPE-1 cells, transfected with siRNAs for 48 h, were serum-starved overnight; they were re-fed with medium containing 5% serum for the indicated time points, then collected immediately for quantitative western blot analysis.

Primary Hepatocyte Isolation and Hippo Inactivation *In Vivo*

The livers from three week-old male C57BL/6 (Jackson Laboratory) were perfused by HBSS with 10 mM EDTA and 10 mM HEPES, followed by a liver digest medium (Invitrogen). Cells were filtered through a 70μm strainer, followed by a percoll gradient, and washed twice in DMEM. For gene expression profiling, hepatocytes were stained with Hoechst33342 (for DNA content) and analyzed

with a BD FACS Aria II SORP. For the EdU incorporation assay animals were injected with EdU (100 mg/kg) intraperitoneally 4 h prior to hepatocyte isolation. Isolated cells were fixed in suspension with 2% PFA and EdU-stained according to the manufacturer's instructions **(**Click-iT EdU Alexa Fluor 488 Cell Proliferation Assay Kit; Life Technologies). Cells were subsequently stained with Hoechst for DNA content and analyzed with a BD LSR Fortessa. To induce YAP S127A expression *in vivo*, three-week-old tetracycline-inducible YAP S127A mice (Camargo et al, 2007), containing Rosa26-lox-STOP-lox-rtTA and Rosa26-lox-STOP-lox-EYFP alleles, were injected with AAV8-TBG-Cre for hepatocyte-specific induction. Doxycycline (1 mg/ml) was provided in the drinking water 7 days after viral delivery; after 7 days of doxycycline treatment, hepatocytes were isolated via collagenase perfusion, stained with Hoechst33342, and FACS-analyzed.

RNA extraction, Reverse transcription and Quantitative PCR

Total RNA from cultured cells, or from freshly isolated hepatocytes, was isolated using the RNeasy kit (Qiagen); cDNA from samples was generated with the Superscript III kit (Invitrogen) and oligo(dT) primers. Quantitative real-time PCR was performed with SYBR Green technology in a Vii 7 detection system (Applied Biosystems). All primers used can be found in the Extended Experimental Procedures.

Reagents and Antibodies

The following antibodies were from Cell Signaling Technologies: AKT (#9272), Phospho-AKT (#4051), Cyclin D1 (#2926), ERK (#9107), Phospho-ERK (#9101), HA-tag (#2367), Phospho-LATS1 (#8654), LATS2 (#5888 and #13646), MST1 (3682), Myosin Light Chain 2 (#3672), Phospho-Myosin Light Chain 2 (#3675), p21 (#2947), YAP (#4912) and Phospho-YAP (#4911). Antibodies against p53 (DO-1), p21 (F-5) and YAP (63.7) were from Santa Cruz. Additional antibodies included p53 (CM-5; Leica Microsystems), LATS2 (A300-479A, Bethyl Laboratories; referred to as anti-LATS, see figure

S3A), TAZ (M2-616, BD Biosciences), MDM2 (IF2, Thermo Scientific), MST2 (EP1466Y, Abcam), RhoA (BK030, Cytoskeleton), Rac1 (102, BD Bioscience) beta-Actin (AC-74, Sigma) and Tubulin (YL 1/2, Novus Biologicals; DM1A, Sigma). Doxorubicin, Dihydrocytochalasin B, and Doxycycline were from Sigma, Sphingosine-1-Phosphate (S1P) was from Cayman Chemical, Lysophosphatidic Acid (LPA) was from Enzo, KU-55933 (ATM inhibitor), and Rac1 inhibitor (553508) was from EMD Biosciences. Taxol was from Invitrogen. Recombinant IGF1 (#8917) was from Cell Signaling Technologies.

Plasmids

Plasmids encoding cDNA for human wildtype YAP (#33091), YAP-S5A (#33093), wildtype RhoA (#12965) and RhoA-Q61L (#12968) were obtained from Addgene. cDNAs encoding human wildtype and kinase-dead (D809A) HA-tagged LATS2 were kindly gifted by A. Hergovich (University College London, UK). YAP-WT, YAP-S5A, LATS2-WT and LATS2-KD were cloned into the pBABE backbone, making use of PCR-based cloning (In-Fusion HD, Clontech). To generate inducible cell lines RhoA-WT and RhoA-Q61L cDNAs were cloned into the Lenti-X Tet-ON 3G system (Clontech).

siRNA Sequences

Dharmacon:

LATS2-1: GCACGCAUUUUACGAAUUC

LATS2-2: ACACUCACCUCGCCCAAUA

LATS2-3: AAUCAGAUAUUCCUUGUUG

LATS2-4: GAAGUGAACCGGCAAAUGC

Qiagen:

LATS2-5: CTGCCACGACTTATTCTGGAA

Dharmacon:

UTR-1: GAGCAGAGUUCUUCUAUUAUU

UTR-2: AAGAAAUGCAGAUGUGUAAUU

Rac1 siRNA was from Life Technologies (#11711). All other siRNAs used in this study were purchased from Dharmacon (siGenome and siSMART Pools). Individual sequences are available upon request.

qPCR Primers

Quantitative real-time PCR was performed with SYBR Green technology in a Vii 7 detection system (Applied Biosystems). The following primer pairs were used:

Actin: CTCTTCCAGCCTTCCTTCCT/AGCACTGTGTTGGCGTACAG

CTGF: CCAATGACAACGCCTCCT/TGGTGCAGCCAGAAAGCT

CYR61: AGCCTCGCATCCTATACAACC/TTCTTTCACAAGGCGGCACTC

INHBA: TTGCCAACCTCAAATCGTGCT/CCCACACTCCTCCACGATCAT

FSTL1: GCAGCAACTACAGTGAAATCC/ATGGCAGTTTCATTCTGTTCC

EDN1: TGTGTCTACTTCTGCCACCT/CCCTGAGTTCTTTTCCTGCTT

GEO Accession Numbers

GSE57864: Microarray gene expression from both diploid and evolved tetraploid RPE-1 and BJ-1 cells

GSE57769 : Microarray gene expression data from diploid and tetraploid hepatocytes

Supplementary References

Camargo, F.D., Gokhale, S., Johnnidis, J.B., Fu, D., Bell, G.W., Jaenisch, R., and Brummelkamp, T.R. (2007). YAP1 increases organ size and expands undifferentiated progenitor cells. Curr Biol *17*, 2054-2060.

Carter, S.L., Cibulskis, K., Helman, E., McKenna, A., Shen, H., Zack, T., Laird, P.W., Onofrio, R.C., Winckler, W., Weir, B.A.*, et al.* (2012). Absolute quantification of somatic DNA alterations in human cancer. Nature Biotechnology *30*, 413-421.

Sabass B, Gardel ML, Waterman CM, Schwarz US. High resolution traction force microscopy based on experimental and computational advances. Biophysical Journal, 94:207–220, 2008.

Tseng Q, Duchemin-Pelletier E, Deshiere A, Balland M, Guillou H, Filhol O, Thery M. Spatial organization of the extra-cellular matrix regulates cell-cell junction positioning. Proceedings of National Academy of Science U S A. 109 (5) 1506-1511, 2012.

Tseng Q, Wang I, Duchemin-Pelletier E, Azioune A, Carpi N, Gao J, Filhol O, Piel M,
Thery M & Balland M. A new micropatterning method of soft substrates reveals that different tumorigenic signals can promote or reduce cell contraction levels. Lab On Chip, 11:2231-40, 2011.

Vignaud T, Ennomani H, Théry M. Polyacrylamide hydrogel micropatterning. Methods in Cell Biology, 120 :93-116, 2014.

Supplemental Figure 1

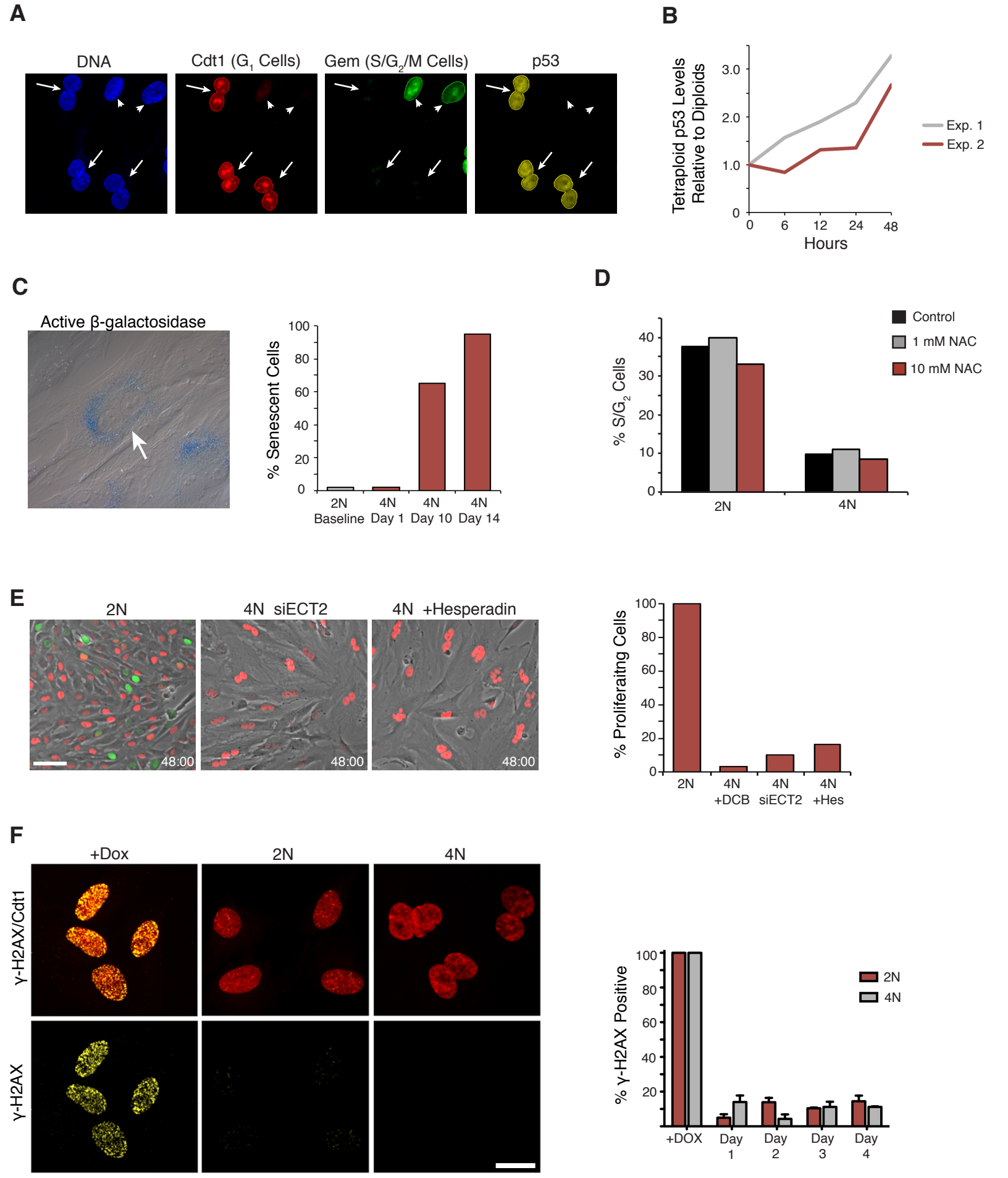

Supplemental Figure 2

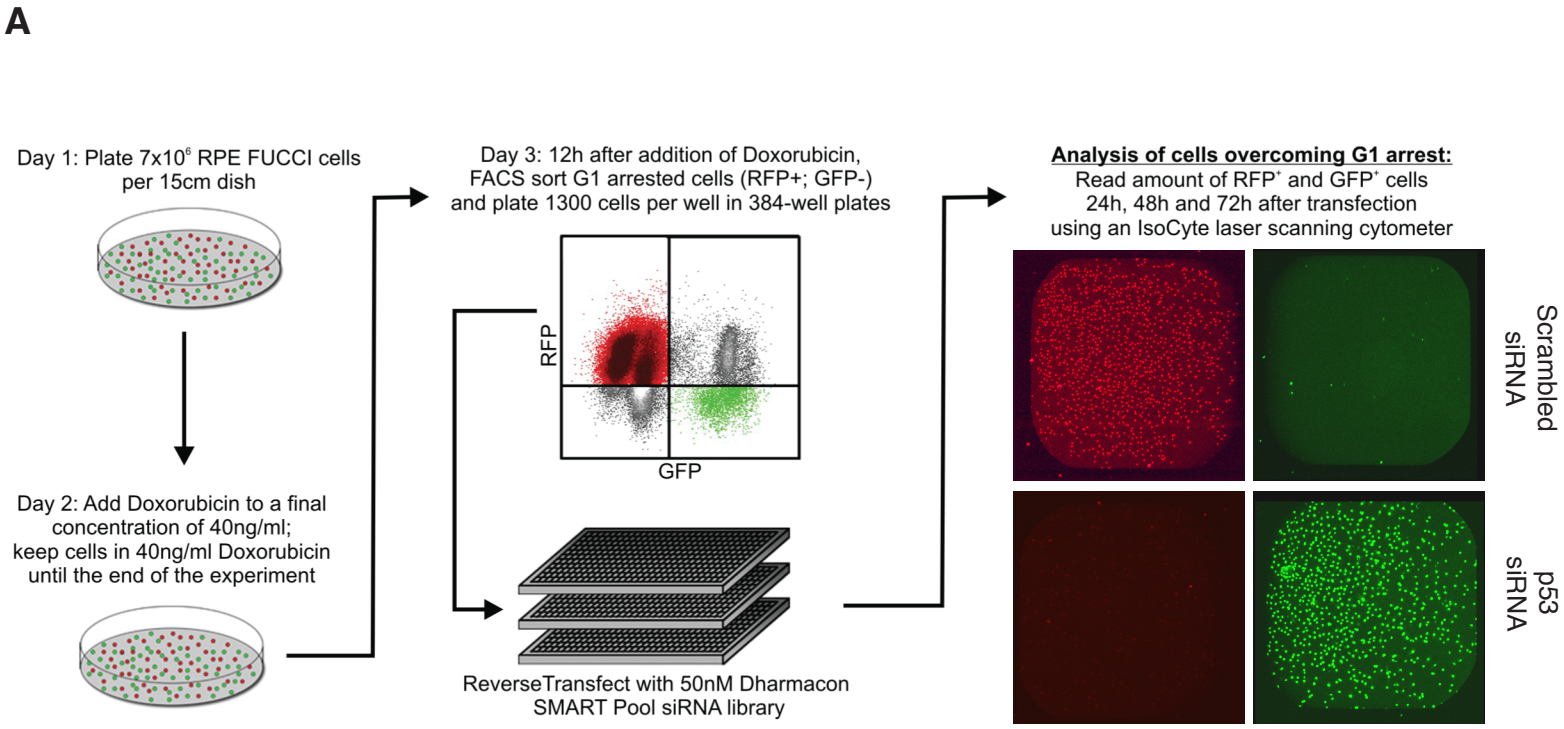

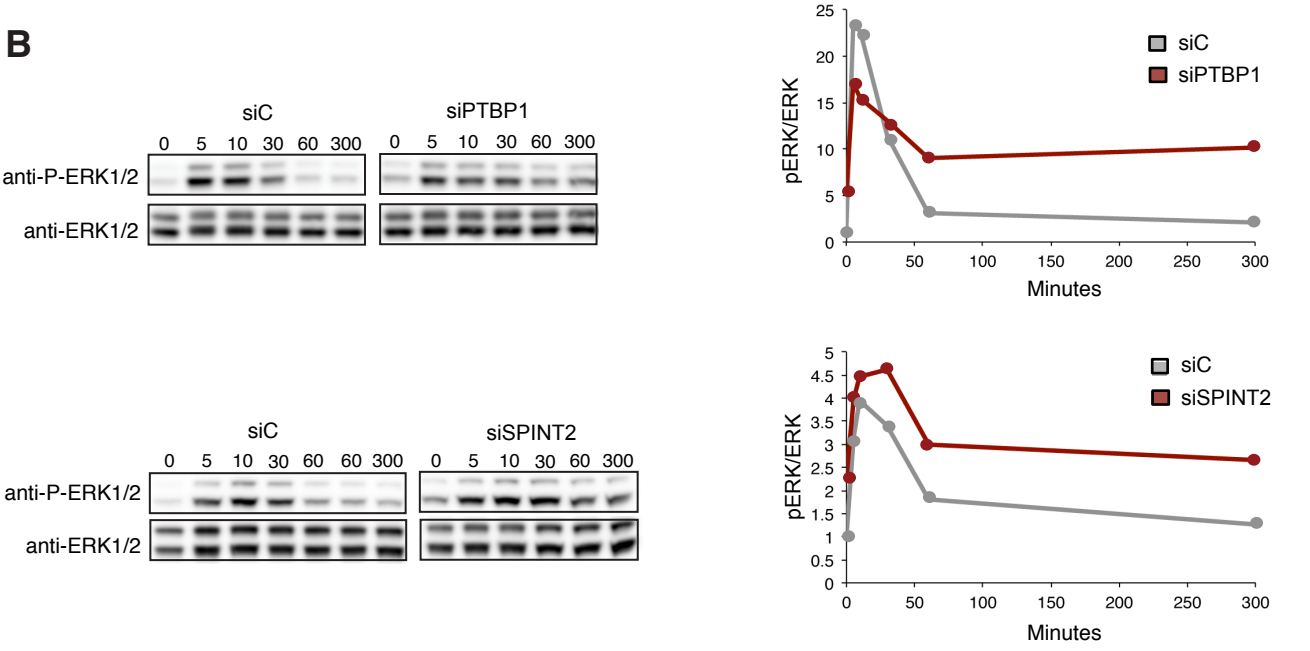

Supplemental Figure 3

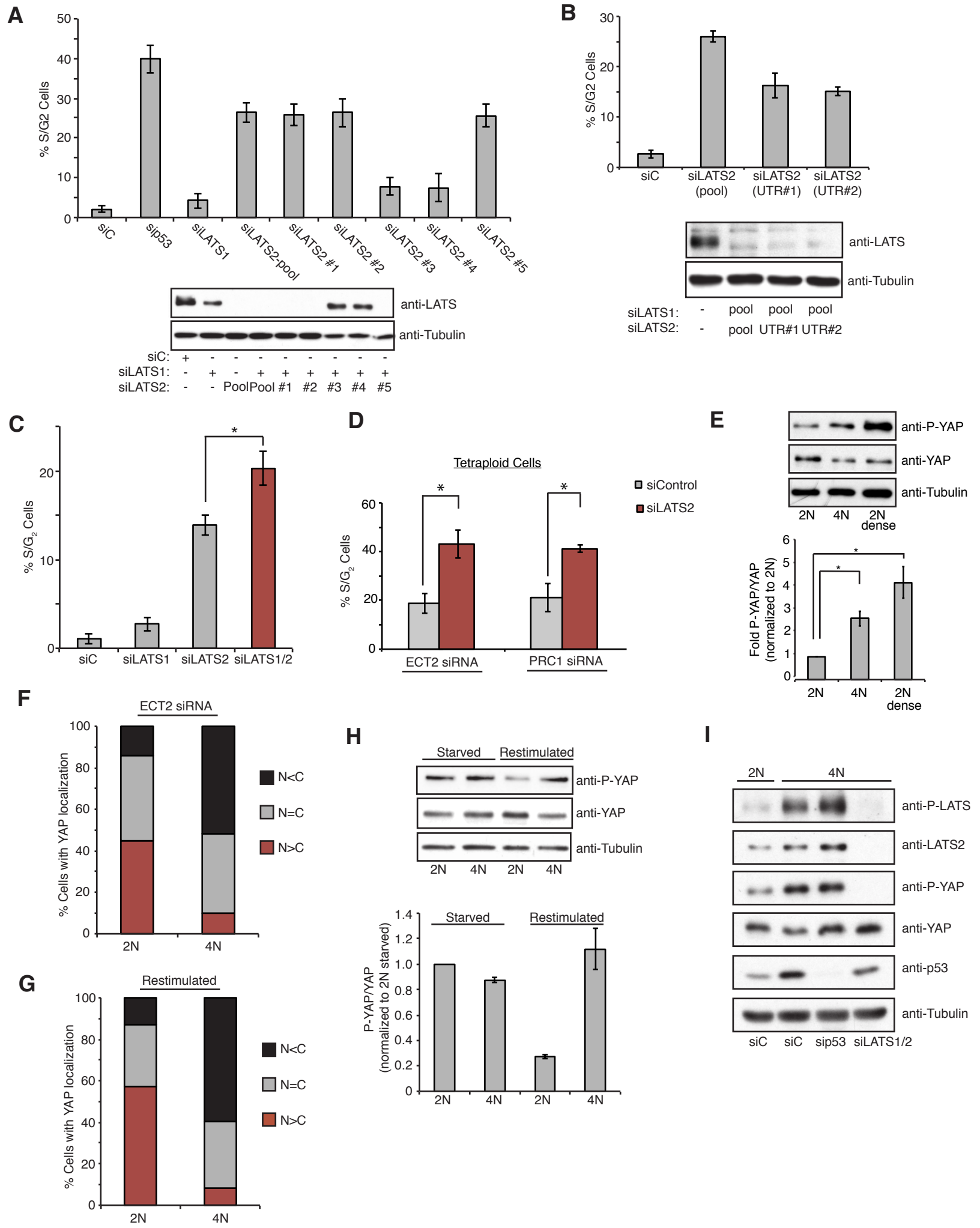

Supplemental Figure 4

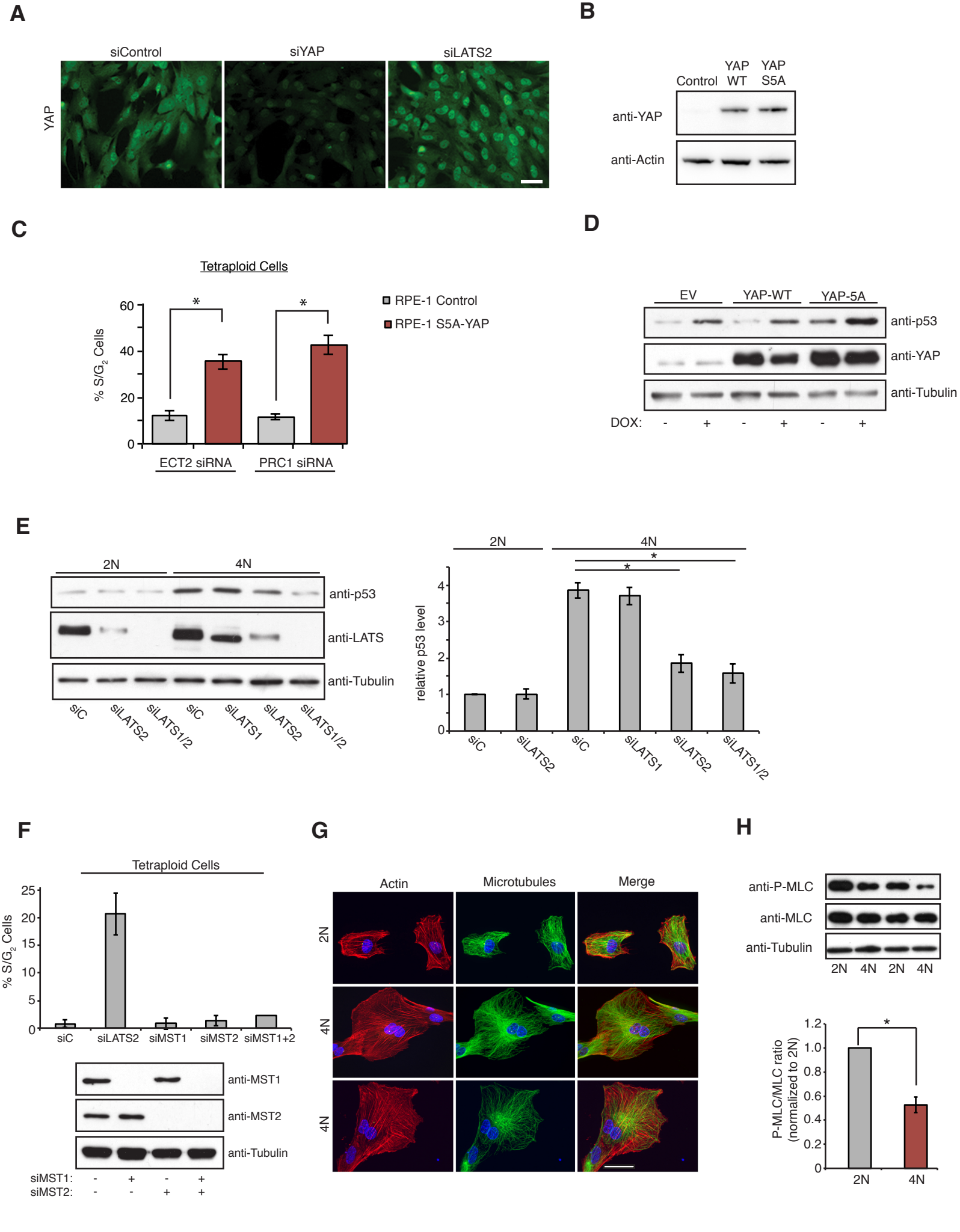

Supplemental Figure 5

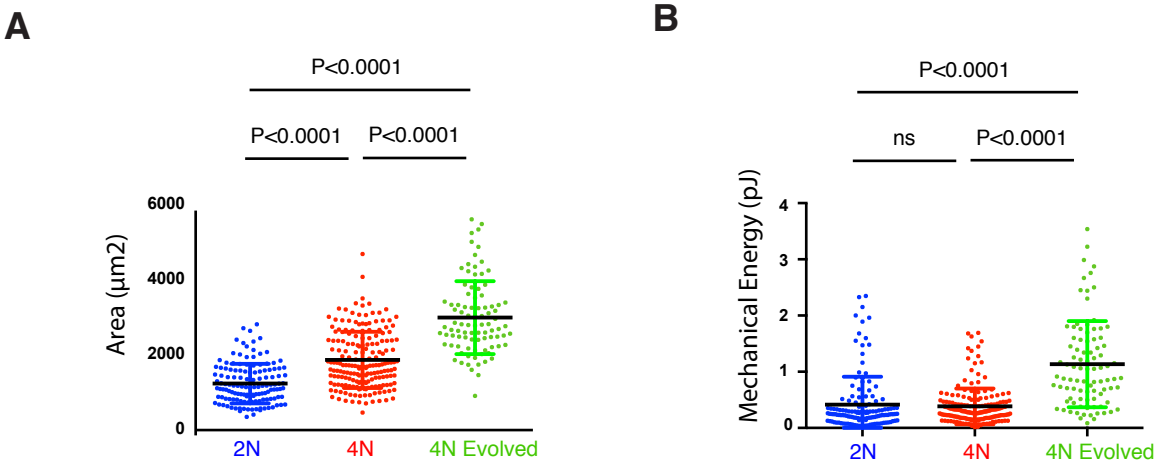

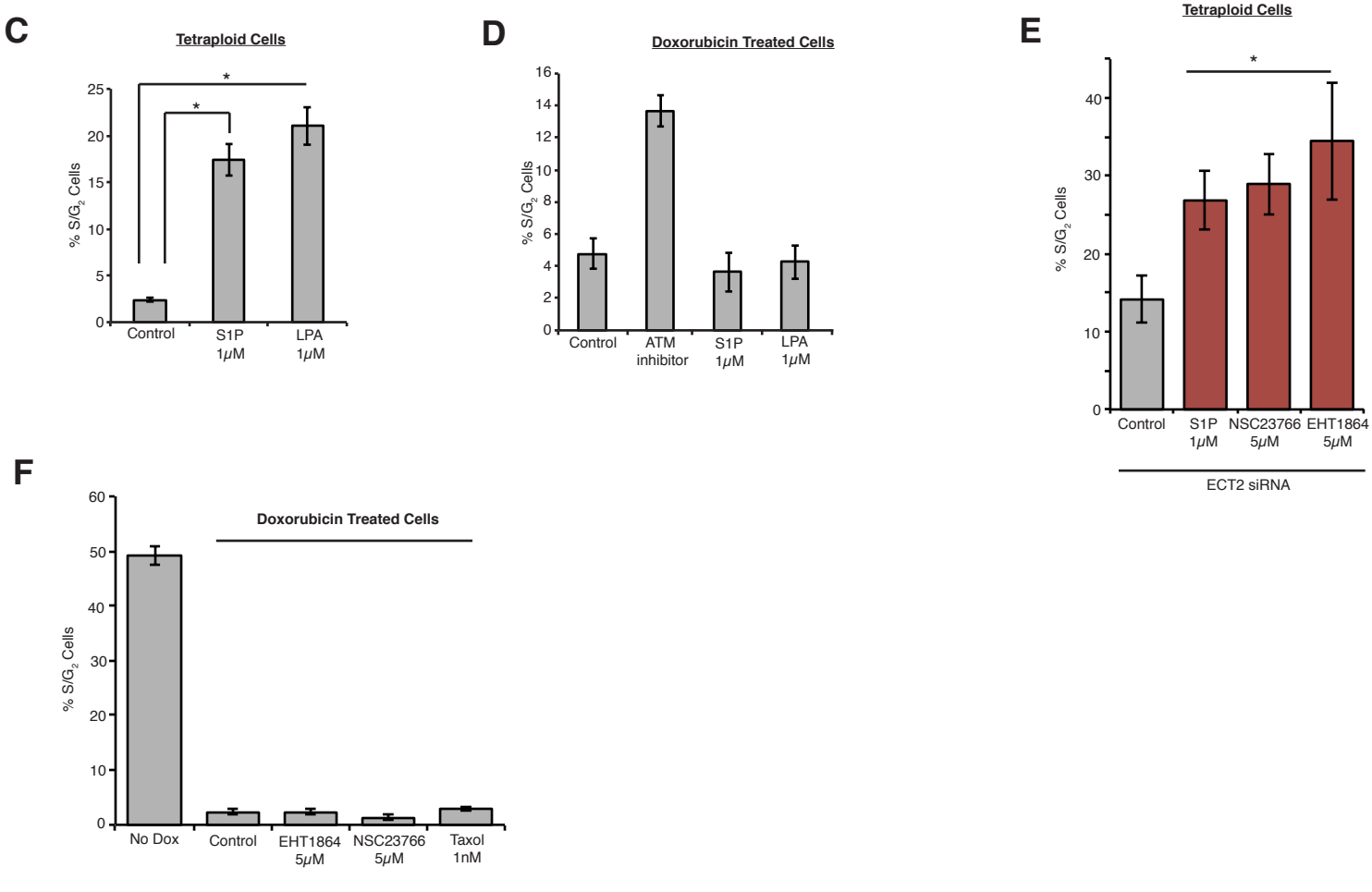

Supplemental Figure 6

A

Geneset	Nominal p-value	FDR q-value	Reference
HIPPO Liver	<0.01	<0.01	Lu et al. PNAS 2010+Dong et al. Cell 2007[a]
YAP/TAZ	<0.0001	<0.0001	Zhang et al. JBC 2009
YAP	<0.005	<0.02	Zhao et al. Genes Dev. 2008

B

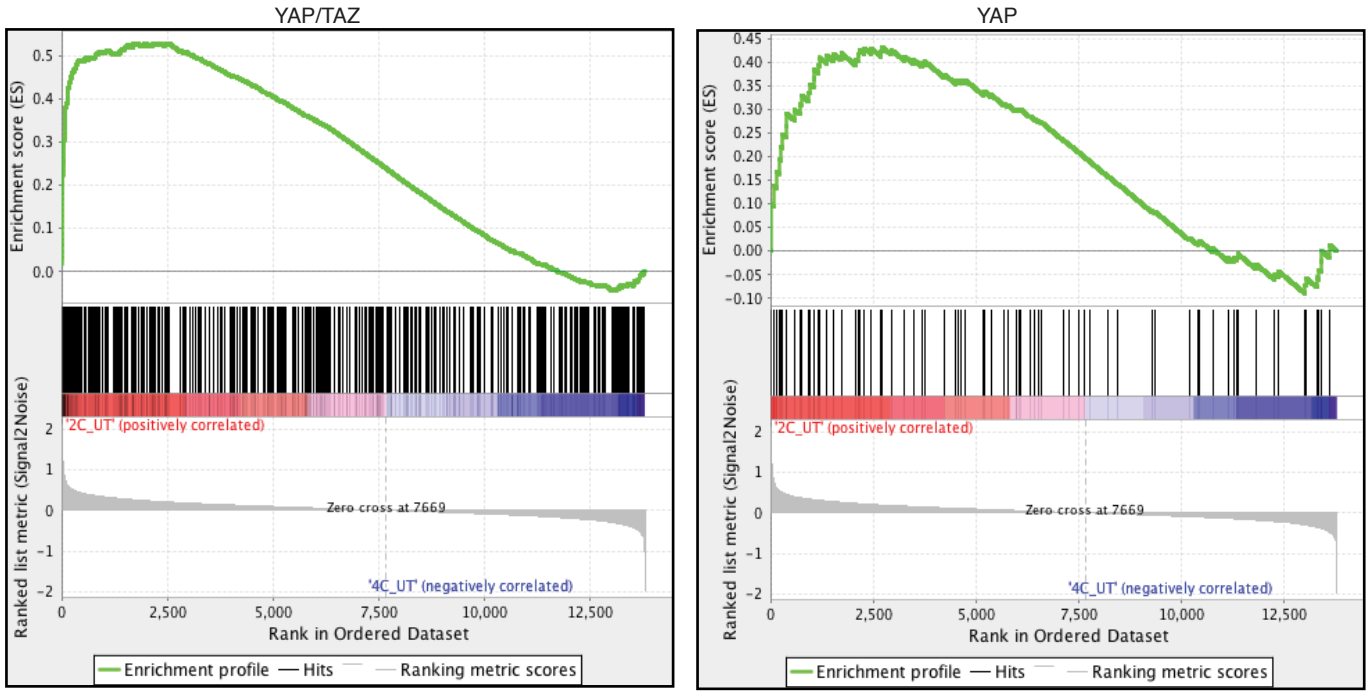

C

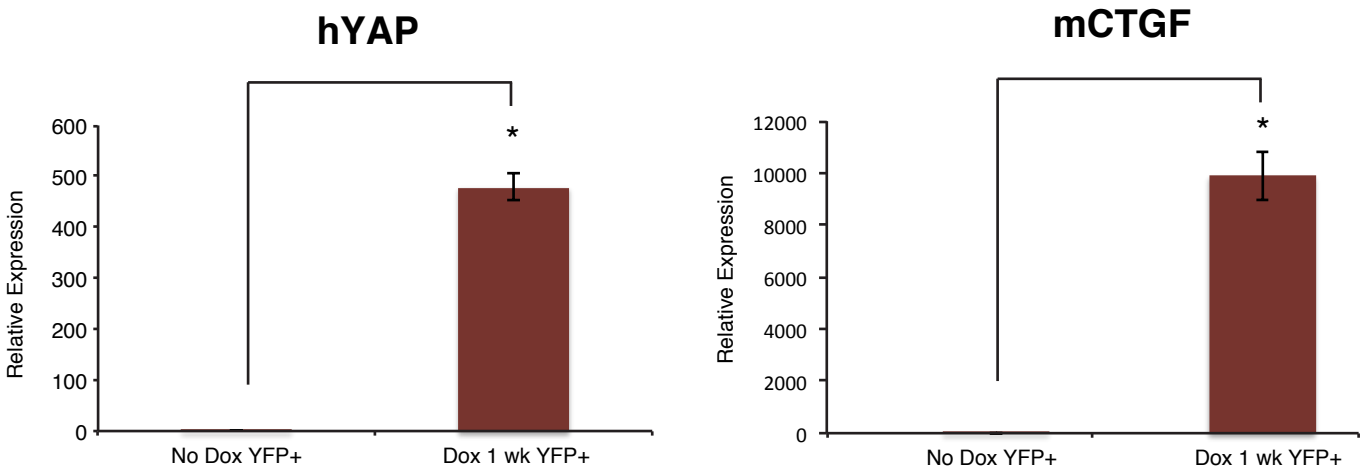

Supplemental Figure 7